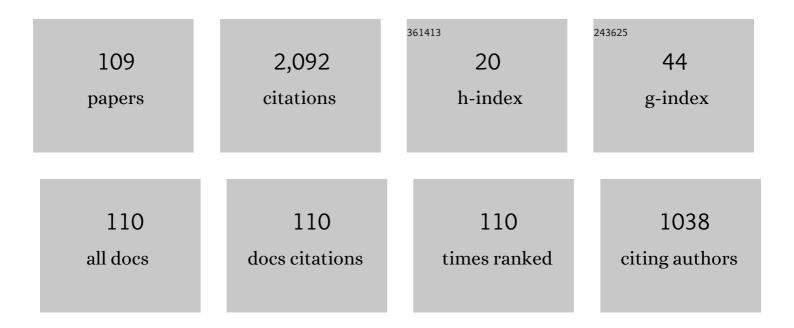


List of Publications by Year in descending order

Source: https://exaly.com/author-pdf/3272645/publications.pdf Version: 2024-02-01



IF # ARTICLE CITATIONS Sub parts-per-billion detection of ethane in a 30-meters long mid-IR Antiresonant Hollow-Core Fiber. Optics and Laser Technology, 2022, 147, 107638. Photodarkening mechanisms of Pr³⁺ singly doped and Pr³⁺/Ce³⁺ 9 3.8 3 coâ€doped silicate glasses and fibers. Journal of the American Ceramic Society, 2022, 105, 3291-3302. Temperature-Dependent Group Delay of Photonic-Bandgap Hollow-Core Fiber Tuned by Surface-Mode 3.4 Coupling. Optics Express, 2022, 30, 222. Study of photodarkening mechanism of Tb3+-activated silica, phosphate, fluorophosphate, and 4 3.6 5 fluoríde glasses. Optical Materials, 2022, 127, 112329. Experimental and numerical analysis of gas flow in nodeless antiresonant hollow-core fibers for 4.6 optimization of laser gas spectroscopy sensors. Optics and Laser Technology, 2022, 152, 108157. Macro- and Microresearch on Swelling Characteristics and Deformation Mechanism of Red-Bed 6 0.7 3 Mudstone in Central Sichuan, China. Geofluids, 2022, 2022, 1-18. Coherent Supercontinuum Generation in Step-Index Heavily Ge-Doped Silica Fibers With All Normal Dispersion. IEEE Photonics Journal, 2022, 14, 1-6. Two-photon endomicroscopy with microsphere-spliced double-cladding antiresonant fiber for 8 3.4 5 resolution enhancement. Optics Express, 2022, 30, 26090. Dynamics of Trace Methane Diffusion/Flow Into Hollow Core Fiber Using Laser Absorption 4.7 Spectroscopy. IEEE Sensors Journal, 2021, 21, 6287-6292. Delivery of CW laser power up to 300 watts at 1080â€...nm by an uncooled low-loss anti-resonant 10 3.4 33 hollow-core fiber. Optics Express, 2021, 29, 1492. Photoionization-Induced Broadband Dispersive Wave Generated in an Ar-Filled Hollow-Core Photonic Crystal Fiber. Crystals, 2021, 11, 180. Laboratory Model Tests on Flow Erosion Failure Mechanism of a Slope Consisting of Anging Group 12 0.7 4 Clay Gravél Layer. Geofluids, 2021, 2021, 1-14. Long-term uplift of high-speed railway subgrade caused by swelling effect of red-bed mudstone: case 3.5 study in Southwest China. Bulletin of Engineering Geology and the Environment, 2021, 80, 4855-4869. Modelling of pressure-driven gas flow in a nodeless Anti-Resonant Hollow Core Fiber for laser 14 0 absorption spectroscopy., 2021,,. Luminescence properties and energy transfer behavior of Dy3+/Tm 3+ co-doped phosphate glasses with 3.1 high moisture-resistance and thermal stability for W-LEDs. Journal of Luminescence, 2021, 236, 118087. A Simulation Study on the Swelling and Shrinking Behaviors of Nanosized Montmorillonite Based on Monte Carlo and Molecular Dynamics. Geofluids, 2021, 2021, 1-13. 16 0.7 1 Inverse Design of Equivalent-Graded-Index Photonic-Crystal Fiber Based on Empirical Dispersion 4.6 Formula. Journal of Lightwave Technology, 2021, 39, 5598-5603. High-efficient subwavelength-scale optofluidic waveguides with tapered microstructured optical 18 3.4 1

Fei Vi

fibers. Optics Express, 2021, 29, 38068.

#	Article	IF	CITATIONS
19	Fabrication of Microchannels in a Nodeless Antiresonant Hollow-Core Fiber Using Femtosecond Laser Pulses. Sensors, 2021, 21, 7591.	3.8	7
20	Spiral scanning fiber-optic two-photon endomicroscopy with a double-cladding antiresonant fiber. Optics Express, 2021, 29, 43124.	3.4	9
21	Emission properties of Pr3+-doped aluminosilicate glasses at visible wavelengths. Journal of Luminescence, 2020, 220, 117013.	3.1	21
22	Visible emission and energy transfer in Tb ³⁺ /Dy ³⁺ coâ€doped phosphate glasses. Journal of the American Ceramic Society, 2020, 103, 6847-6859.	3.8	19
23	Time-Resolved Spectroscopy of Fluorescence Quenching in Optical Fibre-Based pH Sensors. Sensors, 2020, 20, 6115.	3.8	8
24	Antiresonant Hollow-Core Fiber-Based Dual Gas Sensor for Detection of Methane and Carbon Dioxide in the Near- and Mid-Infrared Regions. Sensors, 2020, 20, 3813.	3.8	60
25	Understanding the material loss of anti-resonant hollow-core fibers. Optics Express, 2020, 28, 11840.	3.4	20
26	Photoionization-assisted, high-efficiency emission of a dispersive wave in gas-filled hollow-core photonic crystal fibers. Optics Express, 2020, 28, 17076.	3.4	11
27	Reinforcement Mechanism and Optimisation of Reinforcement Approach of a High and Steep Slope Using Prestressed Anchor Cables. Applied Sciences (Switzerland), 2020, 10, 266.	2.5	12
28	Study of Spectroscopic Properties of Pr3+ and Tb3+-Doped Glasses as Gain Fiber Materials. , 2020, , .		0
29	High fidelity fibre-based physiological sensing deep in tissue. Scientific Reports, 2019, 9, 7713.	3.3	10
30	Dependence of Waveguide Properties of Anti-Resonant Hollow-Core Fiber on Refractive Index of Cladding Material. Journal of Lightwave Technology, 2019, 37, 5593-5699.	4.6	7
31	Attenuation limit of silica-based hollow-core fiber at mid-IR wavelengths. APL Photonics, 2019, 4, .	5.7	54
32	Negative-Curvature Anti-Resonant Fiber Coupling Tolerances. Journal of Lightwave Technology, 2019, 37, 5548-5554.	4.6	7
33	A Step-Index Silicate Nonlinear Fiber With All Normal Flattened Dispersion for Coherent Supercontinuum. IEEE Photonics Journal, 2019, 11, 1-8.	2.0	0
34	Developing Novel Fibres for Endoscopic Imaging and Sensing. , 2019, , .		0
35	Ultraâ€low background Raman sensing using a negativeâ€curvature fibre and no distal optics. Journal of Biophotonics, 2019, 12, e201800239.	2.3	15
36	Step-index fluoride fibers with all-normal dispersion for coherent mid-infrared supercontinuum generation. Journal of the Optical Society of America B: Optical Physics, 2019, 36, 2972.	2.1	6

#	Article	IF	CITATIONS
37	Highly-tunable, visible ultrashort pulses generation by soliton-plasma interactions in gas-filled single-ring photonic crystal fibers. Optics Express, 2019, 27, 30798.	3.4	6
38	Continuously wavelength-tunable blueshifting soliton generated in gas-filled photonic crystal fibers. Optics Letters, 2019, 44, 1805.	3.3	11
39	Ionization-induced adiabatic soliton compression in gas-filled hollow-core photonic crystal fibers. Optics Letters, 2019, 44, 5562.	3.3	10
40	Quasi-phase-matched high-harmonic generation in gas-filled hollow-core photonic crystal fiber. Optica, 2019, 6, 442.	9.3	17
41	Micro-joule level visible supercontinuum generation in seven-core photonic crystal fibers pumped by a 515  nm laser. Optics Letters, 2019, 44, 5041.	3.3	2
42	Continuous-Wave Mid-Infrared Gas Fiber Lasers. IEEE Journal of Selected Topics in Quantum Electronics, 2018, 24, 1-8.	2.9	16
43	Remote monitoring for a high-speed railway subgrade structure state in a mountainous area and its response analysis. Bulletin of Engineering Geology and the Environment, 2018, 77, 409-427.	3.5	7
44	In vivo multiphoton microscopy using a handheld scanner with lateral and axial motion compensation. Journal of Biophotonics, 2018, 11, e201700131.	2.3	11
45	A Double-Cladding Single Polarization Photonic Crystal Fiber and Its Structure Deviation Tolerance. IEEE Photonics Journal, 2018, 10, 1-10.	2.0	1
46	Single-mode solarization-free hollow-core fiber for ultraviolet pulse delivery. Optics Express, 2018, 26, 10879.	3.4	59
47	Photonic crystal fibers: where from, where to?. , 2018, , .		0
48	Double Clad Fiber Improves the Performance of a Single-Ended Optical Fiber Sensor. Journal of Lightwave Technology, 2018, 36, 3999-4005.	4.6	7
49	45W 2 µm Nanosecond Pulse Delivery Using Antiresonant Hollow-Core Fiber. , 2018, , .		4
50	Flexible single-mode delivery of a high-power 2  μm pulsed laser using an antiresonant hollow-core fiber. Optics Letters, 2018, 43, 2732.	3.3	15
51	World-Beating Performance from Hollow Core Fibers. , 2018, , .		0
52	2-micron Pulse compression using gas-filled negative curvature hollow-core fiber. , 2017, , .		0
53	Multimode quasi-phase-matching of high-order harmonic generation in gas-filled photonic crystal fibers. , 2017, , .		0
54	Endoscopic sensing of alveolar pH. Biomedical Optics Express, 2017, 8, 243.	2.9	31

#	Article	IF	CITATIONS
55	Measurement of resonant bend loss in anti-resonant hollow core optical fiber. Optics Express, 2017, 25, 20612.	3.4	40
56	Mid-infrared 1  W hollow-core fiber gas laser source. Optics Letters, 2017, 42, 4055.	3.3	58
57	Low-Loss Silica Hollow-Core Fiber for UV. , 2017, , .		1
58	Gas filled hollow core mid-IR fibre lasers. , 2017, , .		0
59	High harmonic generation in gas-filled photonic crystal fibers. , 2017, , .		0
60	Low loss anti-resonant hollow-core fibers and applications. , 2017, , .		4
61	Continuous-Wave 3.1 μm Gas Fiber Laser with 0.47 W Output Power. , 2017, , .		5
62	Quasi-phase-matched high harmonic generation in gas-filled photonic crystal fibers. , 2017, , .		0
63	Low-Loss Anti-Resonant Hollow-Core Fibers with Single-Mode Performance. , 2016, , .		1
64	Dispersion measurement of microstructured negative curvature hollow core fiber. Optical Engineering, 2016, 55, 116106.	1.0	5
65	Cavity-based mid-IR fiber gas laser pumped by a diode laser. Optica, 2016, 3, 218.	9.3	116
66	Tunable fibreâ€coupled multiphoton microscopy with a negative curvature fibre. Journal of Biophotonics, 2016, 9, 715-720.	2.3	19
67	Femtosecond pulsed laser ablation to enhance drug delivery across the skin. Journal of Biophotonics, 2016, 9, 144-154.	2.3	21
68	Experimental study of low-loss single-mode performance in anti-resonant hollow-core fibers. Optics Express, 2016, 24, 12969.	3.4	44
69	Fugitive methane leak detection using mid-infrared hollow-core photonic crystal fiber containing ultrafast laser drilled side-holes. , 2016, , .		2
70	Negative Curvature Hollow-Core Optical Fiber. IEEE Journal of Selected Topics in Quantum Electronics, 2016, 22, 146-155.	2.9	200
71	Reduced Repetition Rate Yb3+ Mode-Locked Picosecond Fiber Laser With Hollow Core Fiber. IEEE Photonics Technology Letters, 2016, 28, 669-672.	2.5	7
72	Line-tunable CW Lasing of Mid-infrared Acetylene Gas Hollow Core Fiber Laser. , 2016, , .		1

#	Article	IF	CITATIONS
73	Useful Light from Photonic Crystal Fibres. , 2016, , .		1
74	Achieving a 15 μm fiber gas Raman laser source with about 400 kW of peak power and a 63 GHz linewidth. Optics Letters, 2016, 41, 5118.	3.3	51
75	Pulsed and CW Mid-infrared Acetylene Gas Hollow-Core Fiber Laser. , 2016, , .		2
76	High Peak-Power, Narrow Linewidth, 1.5 μ m Fiber Gas Source Generation by Stimulated Raman Scattering of Ethane. , 2016, , .		0
77	High Peak-Power Narrow Linewidth 1.9 μm Fiber Gas Raman Source. , 2016, , .		1
78	About 400 kW Peak-Power, 7.5 GHz Linewidth, 1.5 μm Fiber Gas Raman Source. , 2016, , .		0
79	Gas Sensing with Hollow Core Fiber for Leak Detection and Localization. , 2016, , .		1
80	Reducing Nonlinear Limitations of Ytterbium Mode-Locked Fibre Lasers with Hollow-Core Negative Curvature Fibre. , 2015, , .		4
81	Hollow core fibers for optically pumped mid-IR fiber lasers. , 2015, , .		0
82	Silica hollow core microstructured fibers for beam delivery in industrial and medical applications. Frontiers in Physics, 2015, 3, .	2.1	20
83	Negative curvature fibres: exploiting the potential for novel optical sensors. , 2015, , .		4
84	High energy green nanosecond and picosecond pulse delivery through a negative curvature fiber for precision micro-machining. Optics Express, 2015, 23, 8498.	3.4	55
85	Synchronously Pumped Mid-IR Hollow Core Fiber Gas Laser. , 2015, , .		1
86	High peak power nanosecond and picosecond pulse delivery through a hollow-core Negative Curvature Fiber in the green spectral region for micro-machining. , 2014, , .		2
87	Out of the Blue and into the Black - Silica Fibers for the Mid-IR. , 2014, , .		1
88	Highly birefringent multicore optical fibers. , 2014, , .		0
89	Efficient diode-pumped mid-infrared emission from acetylene-filled hollow-core fiber. Optics Express, 2014, 22, 21872.	3.4	67
90	Efficient 1.9 <i>μ</i> m emission in H ₂ -filled hollow core fiber by pure stimulated vibrational Raman scattering. Laser Physics Letters, 2014, 11, 105807.	1.4	59

#	Article	IF	CITATIONS
91	High-power femtosecond fiber lasers based on self-similar pulse evolution. Proceedings of SPIE, 2014, ,	0.8	0
92	Highly birefringent 98-core fiber. Optics Letters, 2014, 39, 4568.	3.3	17
93	Single-Pass High-Gain 1.9 μm Optical Fiber Gas Raman Laser. Guangxue Xuebao/Acta Optica Sinica, 2014, 34, 0814004.	1.2	0
94	Diode-Pumped Single-Pass Mid-Infrared Fiber Gas Laser. Guangxue Xuebao/Acta Optica Sinica, 2014, 34, 1014002.	1.2	0
95	1.9 μ m Coherent Source Generation in Hydrogen-Filled Hollow Core Fiber by Stimulated Raman Scattering. , 2014, , .		0
96	Silica hollow core microstructured fibres for mid-infrared surgical applications. Journal of Non-Crystalline Solids, 2013, 377, 236-239.	3.1	20
97	Flexible delivery of Er:YAG radiation at 2.94 \hat{l} /4m with novel hollow-core silica glass fibres: demonstration of tissue ablation. , 2013, , .		0
98	Limits of Hollow Core Negative Curvature Fiber. , 2013, , .		0
99	Flexible delivery of Er:YAG radiation at 294 µm with negative curvature silica glass fibers: a new solution for minimally invasive surgical procedures. Biomedical Optics Express, 2013, 4, 193.	2.9	77
100	Spectral attenuation limits of silica hollow core negative curvature fiber. Optics Express, 2013, 21, 21466.	3.4	119
101	Picosecond and nanosecond pulse delivery through a hollow-core Negative Curvature Fiber for micro-machining applications. Optics Express, 2013, 21, 22742.	3.4	96
102	Delivery of high-power nanosecond and picosecond pulses through a hollow-core Negative Curvature Fibre for micro-machining applications. , 2013, , .		1
103	A hollow-core Negative Curvature Fibre for efficient delivery of NIR picosecond and femtosecond pulses for precision micro-machining. , 2013, , .		1
104	Extended Self-Similar Pulse Evolution in a Laser with Dispersion-Decreasing Fiber. , 2013, , .		1
105	Silica Hollow Core Fibers for Mid-IR Wavelengths. , 2013, , .		0
106	Low loss silica hollow core fibers for 3–4 μm spectral region. Optics Express, 2012, 20, 11153.	3.4	357
107	Low Loss (34 dB/km) Silica Hollow Core Fiber for the 3 \hat{l} /4m Spectral Region. , 2012, , .		0
108	On the characteristics of the cone penetration value and its correlation with bearing capacity for		0

Fei	I Y	11
		ч

#	Article	IF	CITATIONS
109	Laser-Induced damage of Anti-Resonant Hollow-Core Fiber for High-Power Laser Delivery at 1 μm. Optics Letters, 0, , .	3.3	5